JOURNAL OF MATERIALS SCIENCE 29 (1994) 3261–3268

Solid-solution range of mullite up to 1800 °C and microstructural development of ceramics

B. SARUHAN, U. VOβ, H. SCHNEIDER
German Aerospace Research Establishment (DLR), Institute for Materials Research, Department of Ceramics, Postfach 90 60 58, Linder Höhe D-51147, Köln, Germany

Tetraethoxysilane (TEOS) and Al-sec-butylate (Al-O-Bu) were used for the sol–gel synthesis of mullite ceramics. The starting materials had bulk compositions corresponding to values between 72 and 78 wt% Al_2O_3, and 28 and 22 wt% SiO_2, respectively, and were calcined at 400 °C (A-series) and 1100 °C (B-series). B-series samples, despite their higher green densities, could only be sintered to about 65–70% TD (theoretical density) at 1650 °C, whereas A-series samples achieve values of about 93–98% TD. Ceramics with relatively high amounts of glass phase from large tabular mullite crystals, which are embedded in a finer-grained mullite matrix. As soon as the bulk Al_2O_3 content increases, equiaxed mullite grains appear and the mean grain size becomes smaller, showing a significant difference between the nucleation and crystal growth mechanisms of mullites formed in samples with the lower and higher Al_2O_3-bulk compositions. Depending on the bulk composition of the samples, the temperature-controlled solid-solution of mullite ranges between about 72.7 and 74.3 wt% Al_2O_3 at 1600 °C and 74.1 and 75.4 wt% Al_2O_3 at 1800 °C, indicating that the solid-solution region bends over towards the Al_2O_3-side of the Al_2O_3-SiO_2 phase diagram.

1. Introduction

Mullite is the only stable crystalline compound in the system Al_2O_3–SiO_2 under atmospheric pressure and at high temperatures. There have been many conflicting ideas concerning the phase diagram, especially on the melting relations and the composition of mullite. The first fundamental investigation carried out by Bowen & Greig [1] in 1924 showed that mullite of the composition $3Al_2O_3 \cdot 2SiO_2$ (71.8 wt % Al_2O_3) melts incongruently at 1810 °C. Several other papers have added strength to the argument for incongruent melting and for the observation that mullite can exist with higher $Al_2O_3 : SiO_2$ ratios than 3 : 2 [2–6]. Other comprehensive investigations have indicated that a congruent melting of mullite exists [5, 7–10]. In a review, Pask [11] provided evidence for stable incongruent melting at 1828 °C as well as for metastable congruent melting of mullite at 1850 °C. Recent studies of the Al_2O_3–SiO_2 phase diagram by Prochazka & Klug [12] postulated that mullite melts incongruently at about 1890 °C, and that the solid-solution range is shifted towards higher Al_2O_3 compositions at higher temperatures [13].

Despite these investigations, carried out on one of the most important phase diagrams for ceramicists, many open questions remain. In particular the width, shape and position of the solid-solution range have not been clearly established. These are of great importance because the microstructural development of mullite depends heavily on the chemical composition and this development, in turn, greatly influences the resulting mechanical properties of mullite ceramics. Previous investigations carried out on mullite mixed crystals have mainly been related to fusion of SiO_2–Al_2O_3 powder mixtures at elevated temperatures and then recrystallization of mullite.

Reliable and correct knowledge of the Al_2O_3–SiO_2 system and the thermal stability of mullite phase in the ceramics produced from precursors would be very helpful for engineers working with this ceramic material. The main aim of this paper is to provide such information on the solid-solution range of mullite between 1600 and 1800 °C with sol–gel derived mullite precursor powders.

2. Experimental procedure

2.1. Powder synthesis

Proportional amounts of Al-sec-butylate (Al-O-Bu) and tetraethoxysilane (TEOS) were diluted with isopropanol alcohol and admixed in the compositions corresponding to bulk oxides: Al_2O_3 in 72, 74, 76 and 78 wt % (60–68 mol %) and SiO_2 in 28, 26, 24 and 22 wt % (32–40 mol %).

Diluted and mixed metal alkoxides were hydrolysed and polymerized with some excess water under acidic conditions (pH = 1.5). Upon water addition, the sol mixture is immediately gelified. On further homogenization by means of a blender, this gel turned to a milky-coloured, fluidic mass which formed a white and flocculent powder after being dried off at 110 °C in a sandbath. All as-received precursor powders are X-ray amorphous, and above about 980 °C crystallization of mullite and a small amount of γ-Al_2O_3 spinel

0022–2461

from the amorphous state takes place. Part of the as-received precursor powders were calcined at 600 °C for 15 h (A-series: A72, A74, A76, A78) and the other part at 1100 °C for 15 h (B-series: B72, B74, B76, B78). As a complementary study, the A-series samples were presintered at 950 °C (AC-series) and 1250 °C (AD-series) for 15 h, prior to sintering at appropriate temperature.

Independent of their compositional differences, the as-calcined (600 °C) A-series precursors were amorphous. The as-calcined (1100 °C) B-series precursors, however, differ in their phase assemblage, depending on their bulk Al_2O_3 content. The sample having the lowest bulk Al_2O_3 content (B72) consists of mullite and some γ-Al_2O_3 (spinel type phase) [14,15]. As the bulk Al_2O_3 content increases (samples B74 to B78), the amount of mullite decreases gradually, whereas the amount of γ-Al_2O_3 increases simultaneously. The sample with the highest bulk Al_2O_3 content (B78) exhibits γ-Al_2O_3 as the only crystalline phase. All as-calcined B-samples also contain some co-existing non-crystalline phase.

The as-received precursor powders consist of agglomerates, sized 5–10 μm, which consist of uniform, spherical and nanometre-sized particles. After calcining at 600 °C for 15 h (A-series), the precursor powders initially maintain this morphology. But on milling in an alcohol and disperser solution, the spheroids disassociate themselves and yield a fine flowing powder. After calcining at 1100 °C for 15 h (B-series), the initial agglomerates are sintered together to form hard and coarse aggregates. This is because 1100 °C falls at the temperature range where a shrinkage of 4% occurs and also mullitization takes place (see Fig. 1.). After grinding by milling, these hard aggregates exhibit a morphology with faceted and irregular shapes. Despite milling, the particle sizes of these powders (B-series) become no finer than 1 μm.

2.2. Processing of compacts

All calcined powders were mixed in a blender with some isopropanol alcohol and 5% disperser, and waxes which help to ease the pressing. The powder mixtures were wet-milled for 15 h with Si_3N_4 balls in a polypropylene jar. Dried and screened powders are die-pressed and consequently CIPed under 1000 bar pressure to bars of 5 × 6 × 85 mm. After degassing at 600 °C to burn out the organic pressing aids, the A-series samples were heated up slowly (30 °C h^{-1}) to 1050 °C and were held at this temperature for 30 min in order to avoid cracking, which is likely to occur because of the high volume changes at 980–1000 °C due to mullite formation. During the first experiments to optimize the sintering conditions, it was observed that the best pore closure and the most uniform microstructural distribution could be realized by presintering at 1050 °C.

The green densities of the A-series samples were about 35% TD (TD = theoretical density) which is rather low. After presintering at 1050 °C, a density of 55% TD was achieved. B-series samples already had a density of 50% TD at the green form. Therefore no pre-sintering was applied, considering no drastic volume changes to take place.

A- and B-series samples were sintered in air with a heating rate of 600 °C h^{-1} at temperatures of 1600, 1650, 1700, 1750 and 1800 °C. The holding time in each case was 2 h.

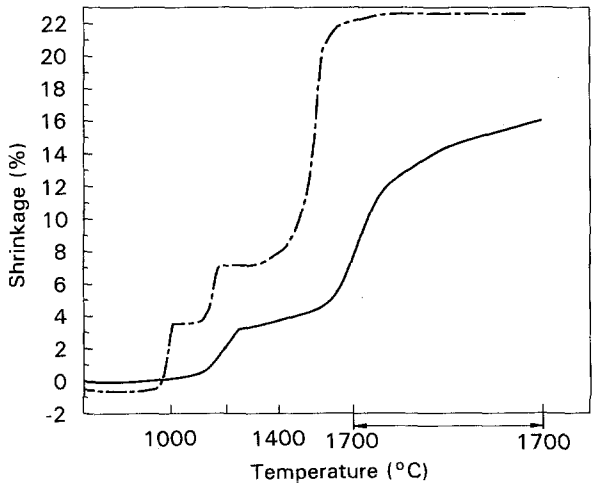

Figure 1 Dilatometer curves obtained with samples (—·—) A74 and (——) B74 (74 wt % Al_2O_3). Measurements were carried in air (heating velocity 20 °C min^{-1}).

2.3. X-ray powder diffraction measurements and determination of lattice parameters

X-ray powder diffraction (XRD) studies were carried out at room temperature with a computer-controlled Siemens D5000 powder diffractometer using Ni-filtered Cu$K_{\alpha 1}$ radiation. Diffraction patterns were recorded in the 10–80°, 2θ range, in the step scan mode (5 s 0.01°, 2θ). As the external standard, the 2θ positions of six silicon peaks were used to correct 2θ positions for the samples. Lattice parameters of mullite were calculated from at least 31 diffraction peaks. A PC computer program was used for lattice parameter refinements. The amount of α-Al_2O_3 (corundum) was determined from the ratio of peak area of 1 1 3 α-Al_2O_3 reflection to the sum of four mullite peaks (2 0 1, 1 2 1, 2 1 1, 2 3 0), as described by Klug *et al.* [13].

2.4. Dilatometer investigations

Dilatometry measurements were carried out in a computer-controlled device equipped with an induction furnace. Measurements were run in air with a heating rate of 20 °C min^{-1}.

2.5. Microstructural investigations

All microstructural investigations were carried out with a Philips 525M scanning electron microscope, following optical microscopy observations of the polished and chemically etched cross-sections.

3. Results

3.1. Sintering behaviour

Typical densification curves of the samples, obtained

from dilatometer measurements, are shown in Fig. 1. Although there is a general tendency of shrinkage with temperature, some stages where the densification is retarded are observed. A-series samples exhibit two distinctive stages of shrinkage inhibition at about 1000 and 1250 °C, whereas the B-series curve displays only one stage at about 1250 °C. According to previous studies by Schneider *et al.* [14], both temperatures refer to intensive mullitization (type I precursor at about 1000 °C, types II and III precursors at about 1250 °C). This determination fits well with the observations that A- and B-series materials are admixtures of type I and type III precursors [14].

The fired densities of the samples in the A-series reach to 97% TD and above for all compositions, with the exception of sample A78. The relative density of the latter at the temperature range of 1650–1800 °C remains between 93 and 96% TD (Table I). All samples in the A-series develop transparency at higher temperatures. In contrast, the samples of the B-series exhibit rather low densities, ranging between 65.7 and 93.6% TD, depending on the bulk composition and sintering temperature (Table II). These display a lower degree of optical transparency than those of the A-series.

3.2. Microstructural development

The comparison of the microstructures in Figs 2 and 3 shows that the microstructural development of mullites in the solid solution range depends on parameters such as the sintering temperature, the bulk composition and the calcination process which may alter the particle size and shape of the powders.

The microstructures of the sintered samples prepared from precursor powders calcined at 600 °C (A-series) and at 1100 °C (B-series), owing to their starting powder morphologies show differences. The grain morphology of the sintered A-series sample with the lowest bulk Al_2O_3 content (A72) is a mixture of elongated and equiaxed grains. The grain lengths at 1650 °C range between 1 and 5 μm and reach 10–20 μm at 1800 °C (Figs 2a and 3a). The sintered B-series samples with the lowest bulk Al_2O_3 content (B72) exhibit an elongated and faceted grain morphology. The length of grains, after sintering at 1750 °C for 2 h, occasionally reaches 30 μm. However, many small grains ranging between 2 and 4 μm can also be observed (Fig. 3b). The grain morphologies of the samples strongly depend on the bulk composition of the materials: as the bulk Al_2O_3 content increases, the grain morphology becomes polygonal and exhibits less elongation. Simultaneously, the grain size decreases considerably and reaches values of < 5 μm in the Al_2O_3-richest sample (A78). The sample with 73% Al_2O_3-content displays a grain morphology at 1750 °C which contains both elongated and polygonal grains, indicating a transitional state in morphology. Samples A76 and A78 contain α-Al_2O_3 as the secondary crystalline phase (Fig. 2c and d). The amount of the secondary crystalline phase decreases with sintering temperature, but its morphology seems to depend greatly on the calcination temperature.

TABLE I Variations of the *a*-lattice distance, the compositional phase assemblage and the relative density with the initial bulk composition and the temperature in the A-series (calcined at 600 °C)

Sample key	Sintering temperature T (°C)	*a*-Lattice constant (Å)	Al_2O_3 in mullite (estimated*) (wt %)	Measured α-Al_2O_3 content (wt%)	Relative density (% TD)
A-72	1600	7.548 (5)	72.9 (0.20)	–	–
	1650	7.547 (1)	72.8 (0.20)	–	97.14
	1700	7.551 (1)	73.3 (0.20)	–	98.41
	1750	7.552 (0)	73.4 (0.20)	–	98.10
	1800	7.556 (1)	74.1 (0.20)	–	99.70
A-73	1650	7.553 (2)	73.6 (0.22)	–	–
	1700	7.553 (2)	73.6 (0.22)	–	–
	1750	7.550 (3)	73.3 (0.20)	–	–
	1800	7.558 (0)	74.2 (0.15)	–	–
A-74	1650	7.558 (0)	74.2 (0.25)	–	98.42
	1700	7.560 (0)	74.4 (0.20)	–	98.10
	1750	7.557 (1)	74.1 (0.20)	–	98.10
	1800	7.560 (0)	74.4 (0.20)	–	99.70
A-75	1650	7.560 (4)	74.4 (0.15)	1.2	–
	1700	7.562 (0)	74.6 (0.15)	t	–
	1750	7.565 (5)	75.1 (0.20)	–	–
	1800	7.560 (0)	74.4 (0.20)	–	–
A-76	1650	7.561 (1)	74.5 (0.20)	4.5	97.82
	1700	7.567 (2)	75.2 (0.22)	3.0	99.06
	1750	7.570 (4)	75.9 (0.30)	2.0	99.06
	1800	7.575 (1)	76.2 (0.22)	t	99.37
A-78	1650	7.554 (3)	74.0 (0.32)	12.5	93.37
	1700	7.566 (0)	75.1 (0.30)	11.4	96.05
	1750	7.568 (0)	75.3 (0.22)	11.0	96.04
	1800	7.570 (2)	75.9 (0.22)	8.0	95.72

* Estimated composition, see Section 2.3.

TABLE II Variations of the *a*-lattice constants, compositional phase assemblage and relative density with initial bulk composition and temperature in the B-series (calcined at 1100 °C)

Sample key	Sintering temperature T (°C)	*a*-Lattice constant (nm)	Al_2O_3 in mullite (wt %)	Measured α-Al_2O_3 content (wt %)	Relative density (% TD)
B-72	1650	0.7546 (1)	72.8 (0.30)	–	67.90
	1700	0.7547 (1)	73.0 (0.20)	–	75.63
	1750	0.7548 (1)	73.1 (0.15)	–	91.60
	1800	0.7558 (1)	74.1 (0.20)	–	93.62
B-74	1650	0.7557 (1)	73.5 (0.20)	–	66.87
B-76	1650	0.7565 (0)	75.0 (0.20)	6.0	68.11
	1750	0.7570 (2)	75.6 (0.25)	1.2	75.62
B-77	1650	0.7566 (1)	75.0 (0.20)	9.0	
	1700	0.7568 (1)	75.3 (0.20)	7.5	
	1750	0.7574 (2)	76.0 (0.20)	5.4	
B-78	1650	0.7565 (1)	75.0 (0.25)	18.9	65.76
	1750	0.7574 (1)	76.0 (0.25)	14.0	77.36

* Estimated composition, see Section 2.3.

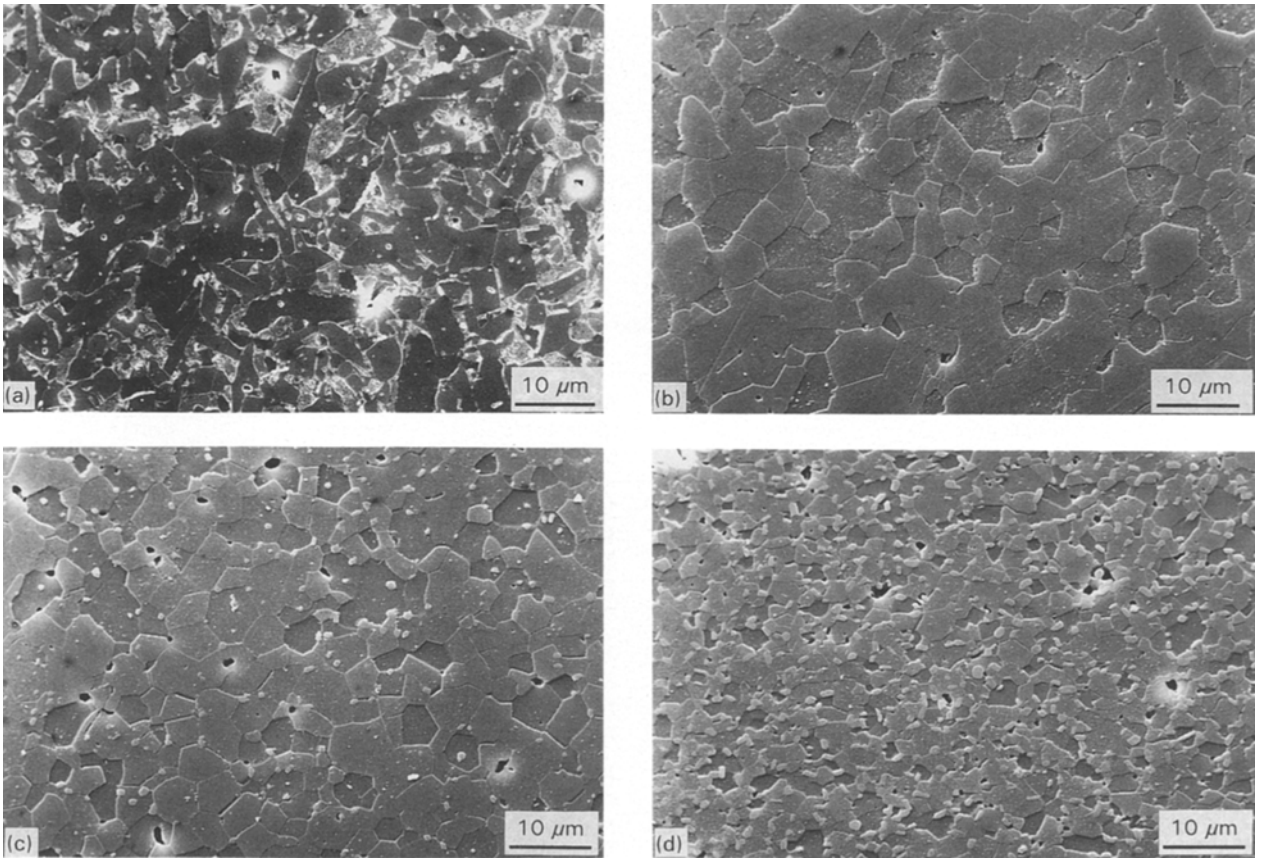

Figure 2 Grain morphology of the samples A72 (a), A74 (b), A76 (c), and A78 (d), sintered at 1650 °C for 2 h (A72: 72 wt % Al_2O_3, A74: 74 wt % Al_2O_3, A76: 76 wt % Al_2O_3, A78: 78 wt % Al_2O_3).

3.3. Lattice parameters and related phase assemblage

The *a*-lattice constants of A-, AC-, AD- and B-series mullites increase with sintering temperature. Figure 4 exhibits the *a*-lattice constant of the mullites obtained at 1250 °C with the all bulk Al_2O_3-contents, prior to further sintering at elevated temperatures. Although the samples compositionally contain an Al_2O_3-content differing from 72 to 78 wt %, the resulting mullites at 1250 °C display a variation in their Al_2O_3-contents from 74.6 to 76.4 wt % (1.8 wt %). The *a*-lattice constants of the A- to B-series exhibit some differences among themselves at a certain sintering temperature, however this variation remains in the given deviations (Tables I to IV). The *b*- and *c*-lattice constants do not change significantly with bulk chem-

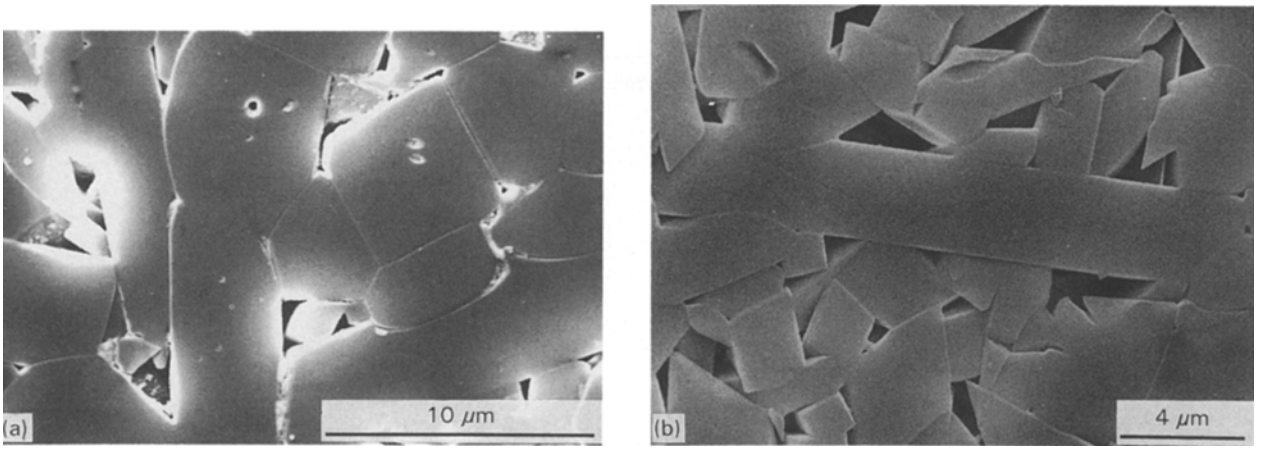

Figure 3 Grain morphology of samples A72(a) and B72(b). Both samples (72 wt % Al_2O_3) were sintered at 1750 °C for 2 h.

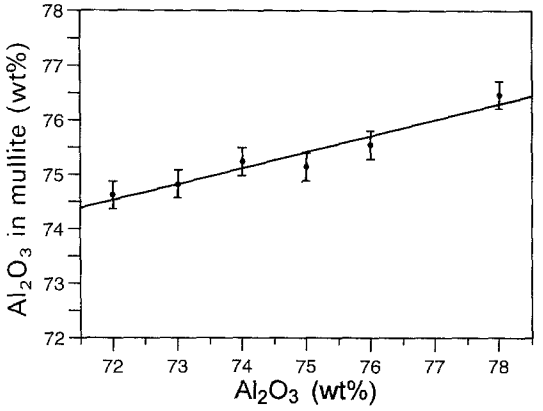

Figure 4 Relation between *a*-lattice constants of mullites and Al_2O_3-contents in mullite obtained at 1250 °C in the samples having various Al_2O_3-bulk compositions.

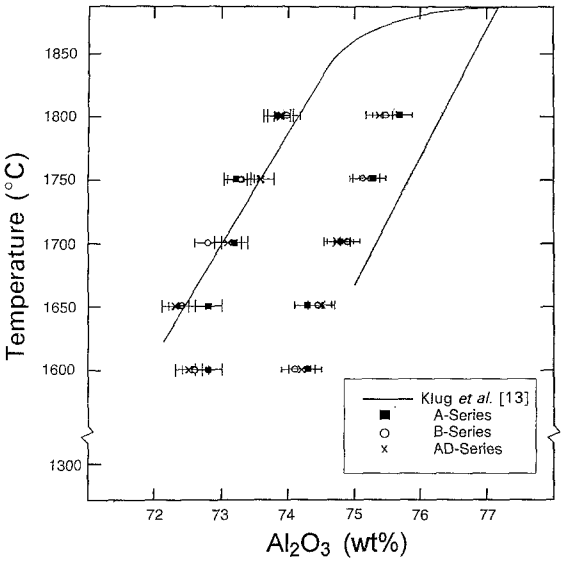

Figure 5 Mullite solid-solution ranges in the Al_2O_3–SiO_2 phase diagram, drawn by using the data from this study (see Tables I to IV). The data of Klug *et al.* [13] are drawn for comparison.

ical composition of samples and with sintering temperature and lie near to *b*: 0.770 and *c*: 0.288 nm, respectively.

Fig. 5 shows Al_2O_3 contents of mullites in the A-, AC-, AD- and B-series, tabulated in Tables I and II, plotted against sintering temperature. The Al_2O_3 contents of mullites were determined from *a*-lattice constants utilizing the curve given by Klug *et al.* [13]. While samples with relatively low bulk Al_2O_3 contents (A72, A74, B72, B74) have only mullite as the crystalline phase, the Al_2O_3-richer samples (A76, A78, B76, B78) after sintering at 1650 °C for 2 h, contain some additional α-Al_2O_3 as secondary crystalline phase. The content of α-Al_2O_3 decreases with increasing temperature at both compositions and series, due to the formation of Al_2O_3-richer mullites (Table I and IV). With increasing temperature, the Al_2O_3-content of mullite generally becomes higher. However, a closer look at the Al_2O_3-contents of mullites in samples having different bulk compositions at the same sintering temperature shows that the Al_2O_3-contents at the samples with the lower Al_2O_3-bulk compositions (up to 74 wt %) increase but with higher Al_2O_3-bulk compositions (above 74 wt %) achieve a constant value at a given sintering temperature (Tables I to IV). For instance, the *a*-lattice constant of the AD-series samples remains on average at 7.5600 Å at 1650 °C, although α-Al_2O_3-content continuously increases with Al_2O_3-bulk content above 74 wt %.

4. Discussion

4.1. Densification

The same as-received precursor powders were used for the production of the starting powders. However, due to their different calcination temperatures (A series: 600 °C, B series: 1100 °C), they develop particles of different composition, size and shape, which in turn cause different levels of sinterability.

The samples of the B-series, despite their higher green densities can only be sintered around 65–70% TD at 1650 °C, whereas those of the A-series achieve values between 93–98% TD. A length shrinkage of 23% is observed at 1700 °C after 2 h of sintering for the sample calcined at 600 °C (A74) and 14% for the sample calcined at 1100 °C (B74). This stands for a relative length shrinkage difference of 9% (volume

TABLE III Variations of the *a*-lattice constants, the compositional phase assemblage and the relative density with the initial bulk composition and the temperature in the AC-series (calcined at 950 °C)

Sample key	Sintering temperature T (°C)	*a*-Lattice constant (Å)	Al_2O_3 in mullite (estimated) (wt %)	Measured α-Al_2O_3 content (wt %)
AC-72	1600	7.545 (2)	72.6 (0.20)	–
	1650	7.544 (1)	72.5 (0.20)	–
	1700	7.546 (2)	72.7 (0.20)	–
	1750	7.552 (0)	73.4 (0.20)	–
	1800	7.558 (5)	74.2 (0.20)	–
AC-73	1650	7.552 (5)	73.4 (0.20)	–
	1700	7.555 (0)	73.7 (0.25)	–
	1750	7.558 (1)	74.2 (0.20)	–
	1800	7.559 (0)	74.3 (0.20)	–
AC-74	1650	7.560 (0)	74.4 (0.15)	–
	1700	7.557 (2)	74.1 (0.20)	–
	1750	7.556 (2)	74.1 (0.20)	–
	1800	7.562 (1)	74.7 (0.20)	–
AC-75	1600	7.558 (0)	74.2 (0.15)	2.0
	1650	7.561 (0)	74.6 (0.15)	1.5
	1700	7.565 (0)	75.0 (0.15)	t
	1750	7.568 (0)	75.2 (0.15)	–
	1800	7.568 (0)	75.2 (0.15)	–
AC-76	1650	7.561 (1)	74.6 (0.25)	6.0
	1700	7.564 (1)	75.0 (0.25)	3.7
	1750	7.568 (1)	75.2 (0.20)	2.3
	1800	7.573 (1)	75.8 (0.20)	–
AC-78	1650	7.558 (2)	74.2 (0.30)	18.2
	1700	7.565 (5)	75.0 (0.25)	15.9
	1750	7.567 (0)	75.1 (0.30)	14.2
	1800	7.572 (0)	75.7 (0.30)	12.0

TABLE IV Variations of the *a*-lattice constants, the compositional phase assemblage and the relative density with the initial bulk composition and the temperature in the AD-series (calcined at 1250 °C)

Sample key	Sintering temperature T (°C)	*a*-Lattice constant (Å)	Al_2O_3 in mullite (estimated) (wt %)	Measured α-Al_2O_3 content (wt %)
AD-72	1600	7.545 (1)	72.6 (0.20)	–
	1650	7.542 (2)	72.4 (0.20)	–
	1700	7.549 (1)	73.0 (0.20)	–
	1750	7.554 (0)	73.6 (0.20)	–
	1800	7.556 (1)	74.1 (0.20)	–
AD-73	1650	7.548 (1)	72.9 (0.20)	–
	1700	7.553 (1)	73.5 (0.25)	–
	1750	7.559 (0)	74.3 (0.20)	–
	1800	7.560 (0)	74.4 (0.20)	–
AD-74	1650	7.556 (0)	74.1 (0.20)	–
	1700	7.557 (1)	74.2 (0.20)	–
	1750	7.565 (1)	74.5 (0.20)	–
	1800	7.562 (1)	74.7 (0.20)	–
AD-75	1600	7.559 (0)	74.3 (0.25)	1.2
	1650	7.563 (0)	74.7 (0.20)	t
	1700	7.563 (1)	74.7 (0.20)	–
	1750	7.567 (0)	75.2 (0.20)	–
	1800	7.567 (1)	75.2 (0.20)	–
AD-76	1650	7.562 (1)	74.7 (0.20)	4.0
	1700	7.564 (1)	74.9 (0.20)	2.5
	1750	7.568 (0)	75.3 (0.20)	1.0
	1800	7.569 (1)	75.5 (0.20)	–
AD-78	1650	7.561 (0)	74.6 (0.25)	11.7
	1700	7.565 (0)	75.1 (0.25)	10.4
	1750	7.569 (2)	75.5 (0.30)	9.1
	1800	7.569 (0)	75.5 (0.25)	7.4

shrinkage of 27%) which fits very well with the density measurements. A possible reason for the low sintering activity of B-series precursors is that these precursors consist of mullite, prior to sintering. Whereas the "unreacted" A-series precursors are non-crystalline. However, it should also be considered that the starting powders of the B-series consist of coarser and irregular shaped particles which also may hinder shrinkage.

The strong influence of the particle size and shape of the precursor powders on the sinterability was stressed by the behaviour of AC and AD samples which were calcined at 400 °C and were presintered at 950 ° and 1250 °C, respectively. Densities as high as 95% TD were achieved after sintering at 1650 °C. This indicates that the majority of densification takes place prior to mullite crystallization (i.e. < 950 °C).

4.2. Microstructural development of mullite ceramics as a function of bulk composition and calcination temperature

Ceramics with relatively low bulk Al_2O_3 contents (i.e. high SiO_3-contents) are associated with relatively high amounts of glass phase and form large tabular mullite grains [16, 17] (Figs 2a, 3a and 3b). As the bulk Al_2O_3 content of the samples increases, the morphology of mullite grains gradually changes to yield a polygonal grain structure with Al_2O_3 bulk compositions > 74 wt % Al_2O_3 (Figs 2a, 2b and 2c). At first glance, this may be connected to the compositional changes observed in mullite crystals. However, it can be postulated that there exists distinct differences in the nucleation and growth mechanisms of the mullite crystals rather than the composition of the mullite crystals as the bulk Al_2O_3 content increases. In fact, these differences should be responsible for the microstructural differences observed in mullite ceramics with various bulk compositions. Furthermore Fig. 4 displays that the compositional difference in mullites formed at 1250 °C lies about 1.8 wt % Al_2O_3, despite initially existing greater difference in the bulk compositions (6 wt % Al_2O_3). Thus, the surrounding amorphous phase remained around mullite nuclei should have different compositions, depending on the bulk composition of a particular sample.

Al_2O_3-poor samples form above ≈ 950 °C a relatively small number of nuclei which grow at the expense of coexisting non-crystalline phase, producing high aspect ratio grains. Above ≈ 1250 °C an additional number of mullite nuclei is formed by reaction of γ-Al_2O_3 with the amorphous phase. The latter gives rise to the development of a fine crystalline matrix in the ceramics under sintering conditions.

In turn, in samples with higher bulk Al_2O_3 contents, a larger number of mullite nuclei may be formed instantaneously at 1250 °C and grow simultaneously in a Al_2O_3 richer phase. Consequently mullite crystal growth is restricted to polygonal and finer grain structures (Fig. 2).

4.3. Mullite solid solution range

Solid solubility ranges of mullite obtained in the present study and that determined by Klug *et al.* [13] are given in Fig. 5. The mullite and mullite + α-Al_2O_3 phase boundary was drawn for the maximum Al_2O_3-solubility in mullite at a given temperature. The mullite and mullite + silica phase boundary was drawn by plotting the corresponding Al_2O_3 contents of mullites, calculated on the basis of X-ray diffraction data. Similar to the findings of Klug and coworkers [13], a bending of the mullite solid solution range at temperatures above 1650 °C to the Al_2O_3-side of the Al_2O_3–SiO_2 diagram was observed. The SiO_2 rich phase boundary is in agreement with the observations of Klug and colleagues [13]. The Al_2O_3 rich phase boundary of the present study lies parallel to the phase boundary found by Klug and colleagues, however, it displays a lower level of alumina solubility in mullite.

The stoichiometric (3/2) composition of mullite can be achieved below 1600 °C only. Above 1600 °C, the mullite gradually becomes richer in Al_2O_3, though the degree of Al_2O_3 increase also depends on the bulk composition of samples.

Previous studies [1–11] on the Al_2O_3–SiO_2 phase diagram carried out by melting powder mixtures followed by supercooling showed that nucleation of α-Al_2O_3 is difficult from the melts. Therefore, in the absence of α-Al_2O_3 nuclei, mullite can be metastably supersaturated with alumina up to 77 wt % Al_2O_3. In the case of mullite ceramics derived from Al_2O_3-rich precursors, things are completely different, due to the presence of α-Al_2O_3 crystals in each case. Thus, the mullite crystals can not be supersaturated by Al_2O_3. This may explain why the mullite and mullite + α-Al_2O_3 phase boundary is shifted towards lower Al_2O_3 contents in the latter case.

Acknowledgements

The authors would like to thank Professor Dr W. A. Kaysser for his continuous support, and H. Hermanns for preparing the technical drawings.

References

1. N. L. BOWEN, and J. W. GREIG, *J. Amer. Ceram. Soc.* **7** (1924) 238.
2. N. E. FILONENKO and I. V. LAVROV, Quoted in: Davis, R. F. and Pask, J. A., in "Refractory Materials. High Temperature Oxides, Part IV: Refractory Glasses, Glass-Ceramics and Ceramics", edited by A. M. Alper (Academic, New York, London, 1971) p. 37–76.
3. E. C. SHEARS and W. A. ARCHIBALD, *Iron Steel* **27** (1954) 61.
4. J. H. WELCH, *Nature* **186** (1960) 545.
5. R. F. DAVIS and J. A. PASK, *J. Amer. Ceram. Soc.* **55** (1972) 524.
6. I. A. AKSAY and J. A., PASK, *ibid.* **58** (1975) 507.
7. N. A. TOROPOV and F. Ya. GALAKHOV, Quoted in: Davis, R. F. and Pask, J. A., in "Refractory Materials. High Temperature Oxides, Part IV: Refractory Glasses, Glass-Ceramics and Ceramics", edited by A. M. Alper (Academic, New York, London, 1971), p. 37–76.
8. N. A. TOROPOV and F. Ya. GALAKHOV, Quoted in *ibid.*
9. N. A. TOROPOV and F. Ya. GALAKHOV, Al_2O_3–SiO_2 system (1964). Quoted in *ibid.*
10. S. ARAMAKI and R. ROY, *J. Amer. Ceram. Soc.* **45** (1962) 229.

11. J. A. PASK, *Ceramics Intern.* **9** (1983) 107.
12. S. PROCHAZKA and F. J. KLUG, *J. Amer. Ceram. Soc.* **66** (1983) 874.
13. F. J. KLUG, S. PROCHAZKA and R. H. DOREMUS, *ibid.* **70** (1987) 750.
14. H. SCHNEIDER, B. SARUHAN, D. VOLL, L. MERWIN and A. SEBALD, *J. Eur. Ceram. Soc.* **11** (1993) 87.
15. T. M. LOW and R. MCPHERSON, *J. Mater. Sci.* **24** (1989) 926.
16. B. E. YOLDAS and D. PARTLOW, *ibid.* **13** (1988) 1895.
17. J. A. PASK and A. P. TOMSIA, *J. Amer. Ceram. Soc.* **74** (1991) 750.

Received 9 February
and accepted 8 October 1993